tion achieved by bedload particles can be given in terms of fractional depth Z_b and relative grain size $D = d/h$ by

$$Z_b = AD\theta^{1/2} \quad (1)$$

where $\theta = sh/Rd$ with $R = 1.65$ for quartz grains in water and the empirical dimensionless coefficient $A \approx 4$ for irregularly shaped particles (*19*). Thus, a meter-sized boulder would have bounced up to several meters above the bed during peak flood conditions. Sediment of this caliber is relatively rare in the LiWu channel, because the schists that dominate the upper catchment produce much finer debris. In extreme floods, such material would travel in turbulent suspension.

In a channel that is steep-walled and parabolic in cross section, the vertical distribution of particles suspended in simple channel flow can be described generally with a single expression (*20*). Mathematical averaging of this expression over the relative depth range $\{Z_b, 1\}$ yields the fractional depth Z_s, above which the concentration of suspended particles of a given size decays significantly from its near-bed maximum nominally taken at Z_b. Thus, Z_s is given by

$$Z_s = \frac{Z_b^P - Z_b}{(1 - P)(1 - Z)} \quad (2)$$

where $P = 2.5\ \theta^{-1/2}$ for medium sand and larger particles. From Eqs. 1 and 2, we find that only particles for which $P < 0.3$ (or $\theta > 70$) would have traveled in significant numbers at elevations greater than 0.3 h or, equivalently, at >4 m above the bed during peak flood. Such particles have diameters of about 2 mm or less. Thus, we propose that maximal wear rates at midlevels of peak flow are due to rare but significant impacts of large boulders saltating along the bed and to more or less continuous abrasion by very coarse sand and finer material in suspension transport.

Spatially averaged erosion of both rock types between December 2000 and December 2001 approached values of 2 to 6 mm year^{-1} and occurred near the base of the channel. These incision rates are in good agreement with independent estimates of long-term exhumation at 3 to 6 mm year^{-1} mentioned above. During the 2000 wet season, in contrast, spatially averaged wear of both rock types locally exceeded 10 mm to a significant degree, with maximal values observed at greater elevations on the channel wall. This work is assumed to be predominantly a result of Supertyphoon Bilis, because other floods failed to reach that high in the channel. The return period for events equal to or greater than Supertyphoon Bilis is estimated to be about 20 years (Fig. 2A) (*14*). Prorated for this frequency, the maximal spatially averaged erosion rates for the 2000 wet season were 5.5 mm year^{-1} for quartzite and 2.3 mm year^{-1} for schist, but corresponding values for the base of the channel were only 1.7 mm year^{-1} for quartzite and 0.3 mm year^{-1} for schist. This suggests that erosion rates associated with exceptional events fail to balance estimates of long-term exhumation rates throughout the active channel. Our data indicate that the lowering of the LiWu valley is driven by relatively frequent flows of low to moderate intensity (*21*) and that rare large floods are more important in widening the bedrock channel than they are in driving down the base level. However, such floods help transmit the effect of accumulated thalweg lowering to adjacent hillslopes.

References and Notes

1. A. D. Howard, W. E. Dietrich, M. A. Seidl, *J. Geophys. Res.* **99**, 13971 (1994).
2. G. S. Hancock, R. S. Anderson, K. X. Whipple, *Geophys. Monogr.* **107**, 35 (1998).
3. N. Hovius, C. P. Stark, H. T. Chu, J. C. Lin, *J. Geol.* **108**, 73 (2000).
4. K. X. Whipple, N. P. Snyder, K. Dollenmayer, *Geology* **28**, 835 (2000).
5. D. P. Finlayson, D. R. Montgomery, B. Hallet, *Geology* **30**, 219 (2002).
6. K. Tinkler, E. E. Wohl, *Geophys. Monogr.* **107**, 1 (1998).
7. J. Lave, J. P. Avouac, *J. Geophys. Res.* **106**, 26561 (2001).
8. L. S. Sklar, W. E. Dietrich, *Geology* **29**, 1087 (2001).
9. L. S. Teng, *Tectonophysics* **183**, 57 (1990).
10. T. K. Liu, S. Hsieh, Y. G. Chen, W. S. Chen, *Earth Planet. Sci. Lett.* **186**, 45 (2001).
11. M. G. Bonilla, *Geol. Soc. China Mem.* **2**, 43 (1977).
12. P. M. Liew, M. L. Hsieh, C. K. Lai, *Tectonophysics* **183**, 121 (1990).
13. J. D. Milliman, J. P. M. Syvitski, *J. Geol.* **100**, 525 (1992).
14. *Hydrological Yearbook of Taiwan, R.O.C.* (Water Resources Bureau, Taipei, Taiwan, 1960–2000).
15. M. J. Selby, *Zeitschr. Geom.* **24**, 31 (1980).
16. L. Sklar, personal communication.
17. The abrasion mill was loaded with 150 g of 6-mm gravel and was run at 1000 rpm.
18. K. X. Whipple, G. S. Hancock, R. S. Anderson, *Geol. Soc. Am. Bull.* **112**, 490 (2000).
19. W. B. Dade, A. R. M. Nowell, *Euromech* **310**, 201 (1994).
20. G. V. Middleton, J. B. Southard, *Mechanics of Sediment Movement* (Society of Economic Paleontologists and Mineralogists, Tulsa, OK, 1984).
21. M. G. Wolman, J. P. Miller, *J. Geol.* **68**, 54 (1960).

22. This study was funded by NSF grant EAR-9903196 to R.L.S. and N.H. K.H. and W.B.D. are supported by the U.K. Natural Environmental Research Council. Thanks to L. Sklar for measuring tensile strength and erodibility of lithologies at our study site and giving feedback on the manuscript; to two anonymous reviewers for their insight and improvements; to M. Chen, S. Dadson, and D. Kitching for invaluable help in the field; and to the Taroko National Park authorities for generous logistic support.

Supporting Online Material

www.sciencemag.org/cgi/content/full/297/5589/2036/DC1
Fig. S1

14 June 2002; accepted 8 August 2002

Uplift in the Fiordland Region, New Zealand: Implications for Incipient Subduction

M. A. House,[1]* M. Gurnis,[1] P. J. J. Kamp,[2] R. Sutherland[3]

Low-temperature thermochronometry reveals regional Late Cenozoic denudation in Fiordland, New Zealand, consistent with geodynamic models showing uplift of the overriding plate during incipient subduction. The data show a northward progression of exhumation in response to northward migration of the initiation of subduction. The locus of most recent uplift coincides with a large positive Bouguer gravity anomaly within Fiordland. Thermochronometrically deduced crustal thinning, anomalous gravity, and estimates of surface uplift are all consistent with ~2 kilometers of dynamic support. This amount of dynamic support is in accord with geodynamic predictions, suggesting that we have dated the initiation of subduction adjacent to Fiordland.

The response of plate boundaries to the initiation of subduction remains a fundamental, unsolved problem in plate tectonics (*1*). Geodynamic models of subduction initiation generally predict the plate over a newly descending slab will be dynamically uplifted during the first few million years after the initiation of convergence (*1*, *2*). The rate of uplift will be proportional to the rate of convergence whereas the amount of uplift will be proportional to the amount of total compression, at least during the early phase of subduction nucleation (*1*). As a consequence of this dynamic support or uplift, a strong positive gravity anomaly would develop on the overriding plate as the base of the crust is progressively uplifted over time.

The apparently young plate boundary adjacent to the Fiordland region of South Island, New Zealand, along with its offshore

[1]Division of Geological and Planetary Sciences, Caltech, Pasadena, CA 91125, USA. [2]Department of Earth Sciences, University of Waikato, Hamilton 2001, New Zealand. [3]IGNS Ltd., Lower Hutt, Private Bag 30368, New Zealand

*To whom correspondence should be addressed. E-mail: mhouse@gps.caltech.edu

continuation, the Puysegur Bank and Puysegur ridge and trench, may represent one of the few regions on Earth where the sequence of tectonic events associated with subduction nucleation can be constrained (*3–6*). This region [see Supporting Online Material (SOM) Text] may currently be in the uplift stage after subduction initiation (*3*). The change in the position of the relative pole of rotation between the Australian and Pacific plates suggests that convergence increased beginning in Middle Miocene times (*7*). There is a narrow oceanic trench offshore of Fiordland which extends southward for a few hundred kilometers, as well as a steeply dipping Benioff zone extending down to 170 km (*8*) and a young [<2 million years ago (Ma)] andesitic volcano to the south (*9*), showing that subduction of the Australian plate beneath Pacific plate is active today. Perhaps most importantly, the largest gravity anomaly in New Zealand lies within Fiordland (Fig. 1) (*3*) (SOM Text). The region cannot be in isostatic equilibrium because Fiordland stands ~1.5 km above sea level and has a large positive Bouguer anomaly. About +50 mGal (where 1 mGal = 10^{-5} m/s^2) of onshore residual can be attributed to stresses within the lithosphere that tilt the Moho upward (*3, 5, 10, 11*). If these stresses were to relax, Fiordland would subside 1 to 2 km and be topographically equivalent to the Campbell Plateau. Yet paleogeographic reconstructions indicate that much of Fiordland experienced continuous uplift beginning in Early Middle Miocene times (*9*), and uplifted marine terraces in southern Fiordland attest to continued uplift in the recent past (*12*).

Plate reconstructions suggest that subduction initiation along the Fiordland-Puysegur segment of the plate margin migrated northward with time (*6, 7, 13*); therefore, it is reasonable to suppose that Fiordland and the Puysegur region represent a continuum in the response of the overriding plate to subduction initiation. If uplift is a fundamental response to subduction initiation, then the current topography of Fiordland may reflect recent uplift in response to subduction initiation.

As the surface is uplifted, topography that develops drives increased erosional exhumation, and local faulting may drive tectonic exhumation of rocks. Thus, evidence for an increase in denudation may serve as a constraint on the timing of subduction-related uplift. Here we use helium and fission track ages of apatite (*14–16*) to record the cooling history of Fiordland as it is exhumed through the upper crust (*17*). These data should reveal whether spatial and temporal patterns of regional exhumation might be related to subduction initiation adjacent to Fiordland.

We obtained helium and fission track cooling ages for samples from vertical elevation profiles, sea level transects in central and southern Fiordland, and one lake-level transect in northern Fiordland (Fig. 1). We also obtained helium ages for three samples from northern Fiordland, at sea level and at elevation. Our results indicate that enhanced exhumation was coincident with or shortly

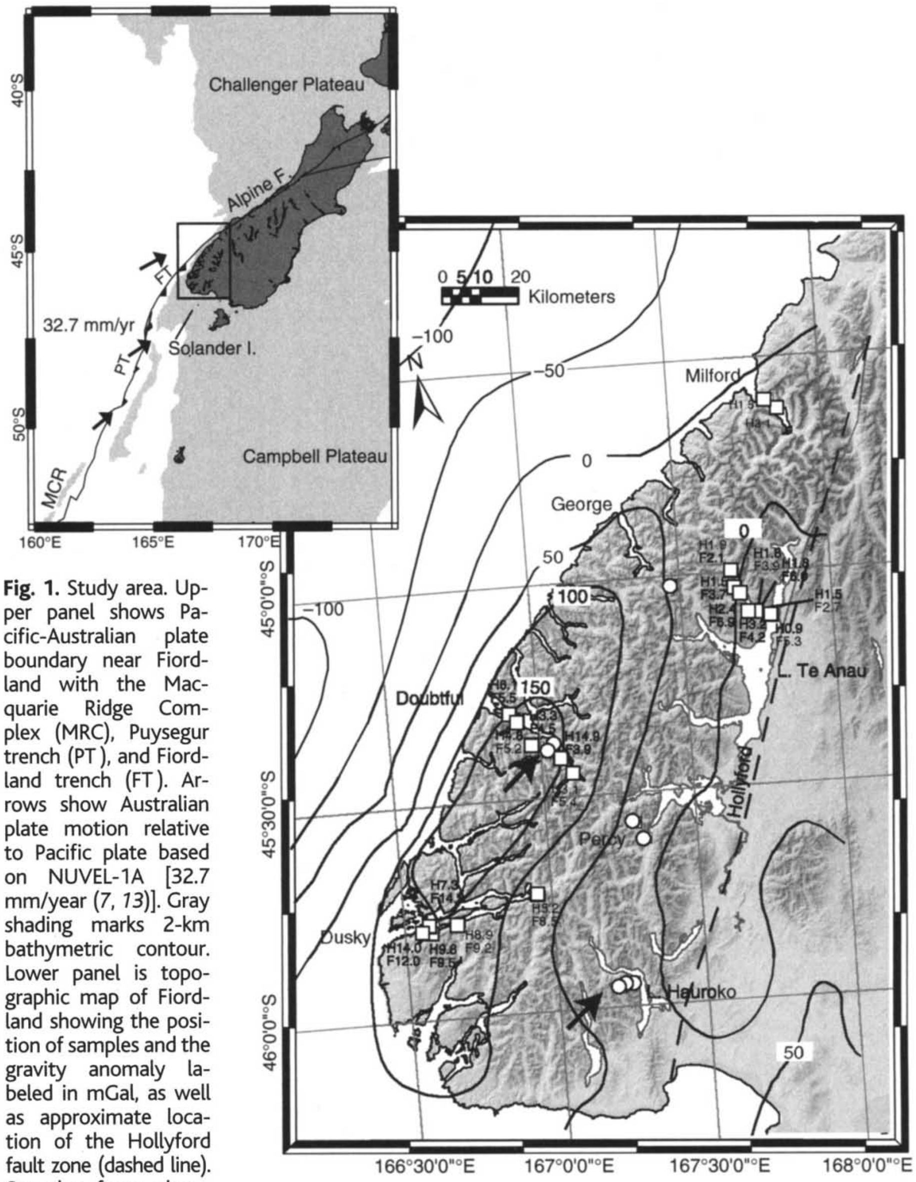

Fig. 1. Study area. Upper panel shows Pacific-Australian plate boundary near Fiordland with the Macquarie Ridge Complex (MRC), Puysegur trench (PT), and Fiordland trench (FT). Arrows show Australian plate motion relative to Pacific plate based on NUVEL-1A [32.7 mm/year (*7, 13*)]. Gray shading marks 2-km bathymetric contour. Lower panel is topographic map of Fiordland showing the position of samples and the gravity anomaly labeled in mGal, as well as approximate location of the Hollyford fault zone (dashed line). Samples from elevation transects are shown with circles; boxes indicate constant elevation transects. Arrows indicate the position of vertical transects at Lake Hauroko and Doubtful Sound. Numbers next to samples along constant elevation transects are helium and fission track ages indicated by "H" and "F," respectively (SOM Text).

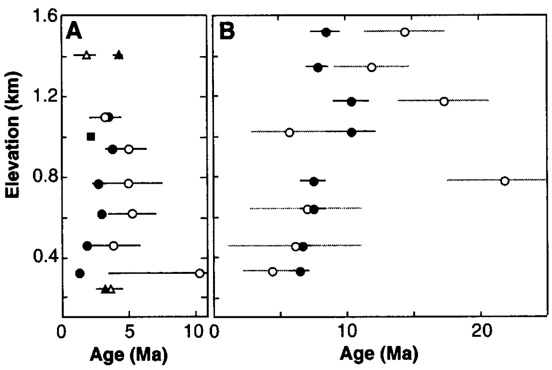

Fig. 2. Helium and fission track data for vertical elevation transects. Helium ages are shown with filled symbols, and fission track ages are shown with open symbols. All ages are shown with 2σ errors. (**A**) Helium and fission track ages from Doubtful Sound (circles), Percy Saddle (triangles), and George Sound (squares). (**B**) Helium and fission track ages from Lake Hauroko.

after the initiation of subduction. Helium and apatite fission track age pairs from elevation transects in central Fiordland are younger than those from the south and show almost no variation in age over about 1.2-km range in elevation (in contrast to the large range in cooling ages over the same approximate elevation range at Lake Hauroko), suggesting that the central region cooled later and more quickly than the southern one (Fig. 2) (*17*). Ages for samples collected at sea level and lake level are also generally younger toward the north (Fig. 3). Helium and fission track ages from Dusky Sound and Doubtful Sound exhibit a systematic decrease in age from west to east as well (Fig. 1). The average helium and fission track ages from each constant elevation transect agree well with results from nearby elevation profiles (Fig. 3).

We used three-dimensional thermal models in which denudation is explicitly tracked using a finite element method to examine the limits on the timing and amount of denudation permissible from fission track and helium ages (*17*). The best-fitting cooling and denudation histories for Doubtful Sound and Lake Hauroko (central and southern Fiordland, respectively) (Fig. 4) indicate: (i) the best-fit exhumation history for Lake Hauroko is slower and initiates earlier than that for Doubtful Sound. (ii) This early episode of denudation accounts for removal of at least 2.5 to 4.5 km of material at Doubtful Sound and ~2.5 to 6 km at Lake Hauroko. (iii) In order to obtain the young helium ages at low elevations in Doubtful Sound, we require a second period of increased denudation (~1.5 to 2.5 km) after ~1.5 Ma. Thus, the total amount of denudation in both areas is at least ~3 to 7 km, but a maximum bound is poorly determined. Though not explicitly modeled, denudation histories inferred for Lake Te Anau, Milford Sound, Georges Sound, Dusky Sound, and Percy Saddle are consistent with these results (SOM Text). Although recent renewed denudation in northern Fiordland is not apparent in southern Fiordland, at least within the resolution of the thermochronometric data, raised marine terraces (*12*, *18*, *19*) attest to continued uplift in the south that may be concomitant with young exhumation in the north.

The onset of rapid exhumation in northern and central Fiordland is not well-constrained from our thermal models. Sedimentologic constraints indicate that about 7 km of exhumation in northern Fiordland began in the Late Miocene (*9*). Our thermal models for Doubtful Sound place a lower limit on the amount and timing of this exhumation to be about 2 to 3 km between 5 to 3 Ma (SOM Text), respectively. Though it is possible that denudation started earlier in the Doubtful Sound region, available sedimentologic and thermochronologic data indicate that it was not coincident with denudation in the south.

We postulate that the observed denudation is directly related to uplift driven by initiation of subduction offshore of Fiordland. Because the Australian plate may have started to thrust beneath the Pacific plate within the last ~12 million years (My) (*3*, *6*), Fiordland would have been uplifted in response to increased convergence during this time (*1*). Plate reconstructions show the boundary between oceanic crust and Challenger Plateau continental crust would have migrated to the north (*3*, *20*), implying that uplift would initiate in the south at Puysegur Bank and slowly migrate to the north as well (SOM Text), with the first phase of uplift in Fiordland occurring at ~11 Ma. This prediction is consistent with the observed pattern of cooling ages indicating that southern Fiordland was exhumed at ~11 Ma, roughly 5 to 7 My earlier than central and northern Fiordland.

Dynamic uplift of Fiordland would be accompanied by the development of a positive Bouguer gravity anomaly centered on the

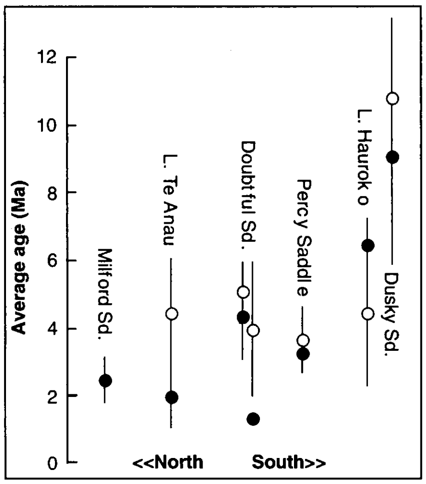

Fig. 3. Average helium and fission track ages for samples from sea level and lake level transects, plotted with lowest elevation samples from Doubtful Sound vertical transect (sample 8901-33, 0.323-km elevation), Lake Hauroko vertical transect (8901235, 0.335-km elevation), and Percy Saddle (8901-53, 0.244-km elevation). Helium ages are shown with filled symbols, and fission track ages are shown with open symbols. Average values (± 1 SD) are for constant elevation transect are as follows: 5.0 ± 0.9 and 4.3 ± 1.3 Ma for Doubtful Sound fission track and helium, respectively; 4.4 ± 1.6 and 1.9 ± 0.9 Ma for Lake Te Anau fission track and helium, respectively; 10.7 ± 2.4 and 9.0 ± 3.2 Ma for Dusky Sound fission track and helium, respectively. Average value for helium ages from Milford Sound is 2.4 ± 0.7 Ma.

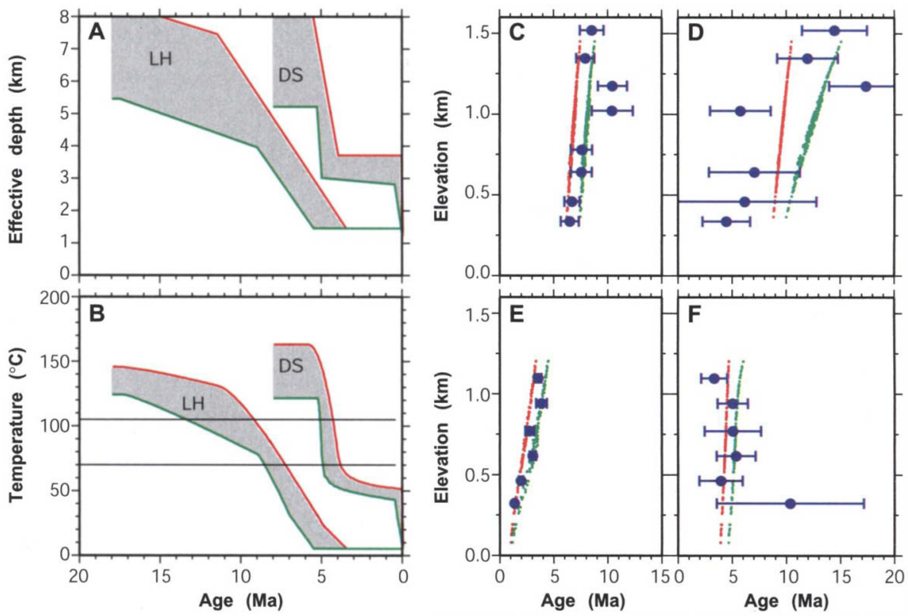

Fig. 4. Thermal models. **(A)** Denudation history plotted as effective depth versus time for Doubtful Sound (DS) and Lake Hauroko (LH), where effective depth = burial depth + modern elevation. For each site, two curves are shown: the red curve indicates the denudation history for the highest elevation sample for each vertical elevation suite that corresponds to a geothermal gradient of 20°C/km, whereas the green curve shows the history corresponding to a geothermal gradient of 30°C/km. **(B)** Time-temperature history computed from denudation histories shown in (A); symbols are as in (A). Thin lines indicate fission track closure isotherm (105°C) and helium isotherm (70°C). **(C)** Model helium ages predicted for range of elevations at Doubtful Sound [all model results are shown in red and green, as in (A) and (B), whereas data from corresponding transects are shown by blue symbols with 2σ errors (Fig. 2)], plotted with observed helium data from Doubtful Sound elevation transect. **(D)** Model fission track ages for Doubtful Sound with observed fission track data from Doubtful Sound elevation transect (Fig. 2). **(E)** Helium ages predicted for Lake Hauroko with observed helium data. **(F)** Model fission track ages for Lake Hauroko, plotted with observed fission track data.

region of greatest and most recent uplift. Indeed, the locus of maximum and most recent uplift that we infer on the basis of thermochronometric data also coincides with the center of the positive Bouguer gravity anomaly beneath Fiordland (Fig. 1).

Assuming a 1 cm/year convergence rate [e.g., (*3*)], about ~1 to 2 km of dynamic support or bedrock uplift within 2 to 4 My of the initiation of subduction is predicted (*1*). The amount of uplift on a continental margin might be larger than 1 to 2 km because erosion in response to uplift of the overriding plate may lead to further isostatic uplift. On the basis of the range of crustal and mantle densities typical for Fiordland crust as well as the fraction of the gravity anomaly due to dynamic support (*5*), the upper crust of central and northern Fiordland must have been thinned by ~7 km to maintain the current average surface elevation and positive gravity anomaly beneath Fiordland. This is similar to the estimate of thinning which we infer based on thermochronometric data from regions coinciding with the gravity anomaly (~4 to 7 km in the Doubtful Sound region), implying that the denudation that we detect and the present day dynamic support of Fiordland have a common origin (SOM Text).

Thermochronologic data from Fiordland record evidence for uplift and exhumation that is temporally related to the inception of subduction offshore of Fiordland. Geodynamic models predict a northward progression in the locus of uplift as subduction propagates northward, which appears to be consistent with denudation tracked thermochronometrically in southern and central-northern Fiordland at ~11 and ~5 Ma, respectively. Although factors like the curved geometry of the Fiordland coast (Fig. 1) and the morphology of the subducted slab below Fiordland (*3*, *20–23*) may play a role in determining how uplift propagates across Fiordland (SOM Text), the agreement between the amount of denudation we observe across Fiordland with the amount of crustal thinning required by the amount of dynamic uplift evident in the gravity signature of the region suggests that these processes are linked. This correlation, coupled with the temporal agreement between enhanced denudation and the onset of subduction offshore of Fiordland implies that we have dated the initiation of subduction along this segment of the Australian-Pacific plate boundary using thermochronometric means (*24*).

References and Notes

1. J. Toth, M. Gurnis, *J. Geophys. Res.* **103**, 18053 (1998).
2. A. I. Shemenda, *J. Geophys. Res.* **97**, 11097 (1992).
3. F. J. Davey, E. G. C. Smith, *Geophys. J. R. Astron. Soc.* **72**, 23 (1983).
4. J. Y. Collot *et al.*, *Eos* **76**, 1 (1995).
5. M. Broadbent, F. J. Davey, R. I. Walcott, *Technical Report No. 124* (New Zealand Department of Scientific and Industrial Research, Lower Hutt, New Zealand, 1978).
6. R. I. Walcott, *Rev. Geophys.* **36**, 1 (1998).
7. C. DeMets, R. G. Gordon, D. F. Argus, S. Stein, *Geophys. J. Int.* **101**, 425 (1990).
8. H. Anderson, T. Webb, J. Jackson, *Geophys. J. Int.* **115**, 1032 (1993).
9. I. M. Turnbull *et al.*, *Technical Report No. 1* (Institute of Geological and Nuclear Sciences, Lower Hutt, New Zealand, 1993).
10. C. M. Ward, *Am. Mineral.* **69**, 531 (1984).
11. P. J. J. Kamp, K. A. Hegarty, *Geophys. J. R. Astron. Soc.* **96**, 33 (1989).
12. D. G. Bishop, *Spec. Publ. Int. Assoc. Sedimentol.* **12**, 69 (1991).
13. C. DeMets, R. G. Gordon, D. F. Argus, S. Stein, *Geophys. Res. Lett.* **18**, 2191 (1994).
14. P. F. Green *et al.*, *Chem. Geol.* **79**, 155 (1989).
15. K. A. Farley, *J. Geophys. Res.* **105**, 2903 (2000).
16. A. J. W. Gleadow, I. R. Duddy, P. F. Green, J. F. Lovering, *Contrib. Mineral. Petrol.* **94**, 405 (1986).
17. Materials and Methods are available as SOM on *Science* Online
18. D. G. Bishop, *N. Z. J. Geol. Geophys.* **28**, 243 (1985).
19. C. M. Ward, *J. R. Soc. N. Z.* **18**, 1 (1988).
20. D. A. Christoffel, W. J. M. Van der Linden, *Ant. Res. Series* **19**, 235 (1972).
21. J.-F. Lebrun, G. D. Karner, J.-Y. Collot, *J. Geophys. Res.* **103**, 7293 (1998).
22. ———, J. Delteil, *Tectonics* **19**, 688 (2000).
23. D. Eberhart-Phillips, M. Reyners, *Geophys. J. Int.* **146**, 731 (2001).

24. Supported by NSF grant EAR-0003558 to M.A.H. and M.G. We thank J. Braun for discussions and J. Braun and T. Ehlers for access to software used in the modeling. Comments from three anonymous reviewers greatly improved the manuscript.

Supporting Online Material
www.sciencemag.org/cgi/content/full/297/5589/2038/DC1
Methods and Materials
SOM Text
Tables S1 to S8
Figs. S1 to S3

21 June 2002; accepted 12 August 2002

An "Endless" Route to Cyclic Polymers

Christopher W. Bielawski, Diego Benitez, Robert H. Grubbs*

A new synthetic route to cyclic polymers has been developed in which the ends of growing polymer chains remain attached to a metal complex throughout the entire polymerization process. The approach eliminates the need for linear polymeric precursors and high dilution, drawbacks of traditional macrocyclization strategies, and it effectively removes the barrier to producing large quantities of pure cyclic material. Ultimately, the strategy offers facile access to a unique macromolecular scaffold that may be used to meet the increasing demand of new applications for commercial polymers. As a demonstration of its potential utility, cyclic polyethylenes were prepared and found to exhibit a variety of physical properties that were distinguishable from their linear analogs.

Produced at a rate of 40 million tons per year, polyethylene remains one of the most valuable synthetic polymers in the world. It is now used in products ranging from grocery bags and milk containers to high-performance fibers and medical devices. Its versatility stems from our ability to tune the material's crystallinity, mechanical strength, and thermal stability by altering the architecture of the individual polymer chains (*1*). However, the rising number of applications for polyethylene require its material properties to be broadened even further. Though most efforts have been focused on synthesizing polyethylene with increasing structural complexity, here we were interested in exploring whether unique properties could be obtained through the simplest of topological modifications; for example, tying the ends of a linear precursor together to form a cyclic polymer conceptually varies the structure only minimally. However, the additional physical constraints imposed on such a cyclic polymer would not only restrict conformational freedom but also reduce its overall dimensions and, therefore, may lead to unusual or unexpected properties.

Although cyclic polymers have been synthesized previously, access to high molecular weight material (MW > 100 kD), which is often required for many polymers to show their characteristic physical properties, is exceedingly challenging (*2*). The typical synthetic route involves intramolecular macrocyclization of linear precursors at extremely low concentrations. Alternatively, the balance between linear and cyclic products that occurs for many polymerizations (e.g., polycondensations, metathesis polymerizations, etc.) may be shifted to maximize formation of cyclic product (which again generally involves using low concentrations). Incomplete cyclizations or undesired side reactions are common for both approaches; therefore, elaborate purification procedures are often required to remove the acyclic contaminants (*3*). Furthermore, many monomers, including ethylene, are not amenable to these types of polymerizations. As a result, there are very few reported examples of cyclic polyeth-

Arnold and Mabel Beckman Laboratories of Chemical Synthesis, Division of Chemistry and Chemical Engineering, California Institute of Technology, Pasadena, CA 91125, USA.

*To whom correspondence should be addressed.